Available online at www.sciencedirect.com
SCIENCE DIRECT®
International Journal of Mass Spectrometry 242 (2005) 257–272
International Journal of Mass Spectrometry
www.elsevier.com/locate/ijms

An assessment of the accuracy of stable Fe isotope ratio measurements on samples with organic and inorganic matrices by high-resolution multicollector ICP-MS

Ronny Schoenberg*, Friedhelm von Blanckenburg

Institut für Mineralogie, Universität Hannover, Callinstrasse 3, 30167 Hannover, Germany

Received 1 October 2004; accepted 30 November 2004

Abstract

Multicollector ICP-MS-based stable isotope procedures provide the capability to determine small variations in metal isotope composition of materials, but they are prone to substantial bias introduced by inadequate sample preparation. Such a "cryptic" bias is not necessarily identifiable from the measured isotope ratios. The analytical protocol for Fe isotope analyses of organic and inorganic materials described here identifies and avoids such pitfalls. In medium-mass resolution mode of the ThermoFinnigan Neptune MC-ICP-MS, a 1-ppm Fe solution with an uptake rate of 50–70 μL min^{-1} yielded 3×10^{-11} A on ^{56}Fe for the ThermoFinnigan stable introduction system and $1.2–1.8 \times 10^{-10}$ A for the ESI Apex-Q uptake system. Sensitivity was increased again 3–5-fold when using Finnigan X-cones instead of the standard H-cones. The combination of the ESI Apex-Q apparatus and X-cones allowed the determination of the isotope composition on as little as 50 ng of Fe. Fe isotope compositions were corrected for mass bias with both the standard-sample bracketing (SSB) method, and by using the $^{65}Cu/^{63}Cu$ ratio of added synthetic copper (Cu-doping) as internal monitor of mass discrimination. Both methods provide identical results on high-purity Fe solutions of either synthetic or natural samples. We prefer the SSB method because of its shorter analysis time and more straightforward correction of instrumental mass bias compared to Cu-doping. Strong error correlations of the data are observed in three isotope diagrams. Thus, we suggest that the quality assessment in such diagrams should be performed with error ellipses rather than error bars. Reproducibility of $\delta^{56}Fe$, $\delta^{57}Fe$ and $\delta^{58}Fe$ values of natural samples alone is not a sufficient criterion for accuracy. A set of tests is lined out that identify cryptic matrix effects and ensure a reproducible level of quality control. Using these criteria and the SSB correction method, we determined the external reproducibilities for $\delta^{56}Fe$, $\delta^{57}Fe$ and $\delta^{58}Fe$ at the 95% confidence interval from 318 measurements of 95 natural samples to be 0.049, 0.071 and 0.28‰, respectively.

Keywords: Fe isotopes; Matrix effects; Stable isotope fractionation; Multicollector ICP-MS

1. Introduction

Stable iron isotopes have been predicted to change their relative abundances in a mass-dependent way by physical transport processes and chemical reactions [1–3]. Indeed, Fe isotope fractionation of up to a few permil per atomic mass unit have been observed in a number of natural and synthetic materials [4–9]. Early attempts to determine stable Fe isotope ratios by thermal ionisation mass spectrometry (TIMS) were hampered by relatively unpredictable instrumental mass discrimination between independent runs of the same sample [10,11]. Nevertheless, high-precision TIMS analyses of stable Fe isotope ratios were accomplished by measuring Fe as negative Fe-fluoride complex, thereby improving the stability of isotopic fractionation between and within runs [12]. The large instrumental mass bias drift typical for TIMS instruments was accounted for by a double-spike technique to

* Corresponding author. Tel.: +49 511 762 5998; fax: +49 511 762 701 0252.
E-mail address: r.schoenberg@mineralogie.uni-hannover.de (R. Schoenberg).

1387-3806/$ – see front matter © 2004 Elsevier B.V. All rights reserved.
doi:10.1016/j.ijms.2004.11.025

further improve the accuracy of stable Fe isotope ratio measurements [13].

With the development of multiple-collector inductively coupled plasma mass spectrometers (MC-ICP-MS) and their advantage of stable mass bias with little drift within and between runs, high-precision isotope ratio determinations were reported for many metals, amongst them Fe [14–18]. However, the accuracy and precision of stable isotope ratio determinations of transition metals by MC-ICP-MS depend on three analytical requirements: (1) the quantitative removal of molecular interferences (e.g. Ar-oxides, Ar-nitrides, Ar- and metal hydrides); (2) accurate corrections for even smallest amounts of isobaric elemental interferences (e.g. $^{54}Cr^+$ on $^{54}Fe^+$, $^{58}Ni^+$ on $^{58}Fe^+$, $^{64}Ni^+$ on $^{64}Zn^+$, etc.); and (3) precise correction of the instrumental mass bias that usually amounts to a few % per atomic mass unit in ICP-MS and that strongly depends on the instrumental set-up, the matrix, and the overall purity in which elements are presented. A number of techniques have been applied to reduce interfering molecular complexes on Fe isotopes, including (i) reduction of H_2O in the aerosol by desolvating nebulisation in order to minimise the $^{40}Ar^{16}O^+/^{56}Fe^+$, $^{40}Ar^{17}O^+/^{57}Fe^+$, and $^{40}Ar^{18}O^+/^{58}Fe^+$ ratios as well as the corresponding Ar-hydroxide and Fe-hydride to iron ratios [15,19]; (ii) A combination of (i) with cool plasma running conditions and the use of a $10^{10}\,\Omega$ resistor for detection of large $^{56}Fe^+$ beams, thereby further minimising the argon-oxide to iron ratio [7]; (iii) collision cell technology [14]; (iv) full suppression of molecular interferences by cold plasma ICP-MS [20]; and (v) high mass resolution measuring techniques [21–24], in order to resolve Fe^+ from ArO^+ and ArN^+ molecules. Isobaric metal interferences are principally removed during chemical purification of the element of interest. Residuals that are not resolvable ion-optically due to their small mass differences may be accounted for by simultaneously monitoring the abundance of another isotope of the interfering element. A variety of approaches exist for the determination of the instrumental mass bias for stable Fe isotope ratio measurements. Most commonly used is the standard-sample bracketing method, SSB (e.g. [7,14,15]), in which measurements of standards of known Fe isotope composition are alternated with measurements of the samples. A second approach derives the instrumental mass bias from simultaneous measurement of additions of Cu [20,25] or Ni [22,23] of known isotope composition. A third approach is a double-spike technique that enables simultaneous calculation of the instrumental mass bias and the sample's natural isotope fractionation. This technique has been used to measure stable Fe isotopes by TIMS [13], but it has not yet been applied to Fe measurements by MC-ICP-MS.

Compared to analyses by multicollector magnetic sector TIMS, MC-ICP-MS techniques improved the precision of stable Fe isotope ratio determinations by a factor of approximately 3–5. The currently reported reproducibility levels are 0.1–0.15‰ (2σ) for $\delta^{56}Fe$ [14,20,23,25], defined as

$$\delta^{56}Fe_{Sample} = \left(\frac{^{56}Fe/^{54}Fe_{Sample}}{^{56}Fe/^{54}Fe_{Standard}} - 1 \right) \times 1000\,[‰] \quad (1)$$

Reproducibilities for Fe isotope determinations at such levels, however, still render some applications impossible, such as measurement of potential high-temperature iron isotope fractionation that was proposed for magmatic processes from spectroscopic data [2,3]. At a precision level of <0.2‰, isotope ratios measured by MC-ICP-MS are easily biased by introduction of "cryptic" matrix effects during analysis. These are, for example, generated by the presence of residual matrix elements in the analyte solution that were not fully disposed of during the chemical purification of the element of interest. The result would be an additional mass bias and a shift in the samples isotope ratios. Such a shift is not readily apparent, it might not even be detected by duplicate measurements [14], since these matrix effects would duplicate, too. Therefore, particularly close scrutiny of instrumental accuracy and precision is required to avoid these pitfalls.

In this study, we used a ThermoFinnigan Neptune MC-ICP-MS situated at the Institute for Mineralogy in Hannover to assess optimal analytic conditions for stable Fe isotope ratio measurements. Molecular interferences are resolved routinely by increasing mass resolution on this instrument [21]. Here we focus on an evaluation of the following aspects that we regard as essential for accurate Fe isotope analyses: (i) assessment of the highest achievable mass spectrometric reproducibility on a synthetic, matrix-free Fe solution; (ii) comparison of standard-sample bracketing with Cu-doping techniques to correct for instrumental mass discrimination; (iii) testing a widely used chromatographic technique for quantitative Fe separation from samples with varying matrices (organic as well as inorganic); (iv) critical assessment of the accuracy and the external reproducibility of the Fe isotope composition of natural Fe samples with organic and inorganic matrices; and (v) following the results from (i) through (iv), establishing a routine analytical protocol for Fe purification and Fe isotope analysis that allows for high confidence in long-term reproducibility and accuracy of stable Fe isotope measurements.

2. Experimental

2.1. Measuring techniques

2.1.1. Instrumentation

The ThermoFinnigan Neptune MC-ICP-MS is a double-focussing sector mass spectrometer equipped with a fixed central channel that can be switched between a Faraday and a secondary electron multiplier detector and four movable Faraday collectors on either side. Varying the width of the entrance slit allows for two different degrees of increased mass resolution (dubbed "medium" and "high" mass res-

olution [21]), thus enabling Fe isotope ratio measurements by fully resolving rather than suppressing the interfering argon-oxides from the Fe isotope masses. The mass resolution is a measure of the relative width of an ion beam and as such for the resolving power of an instrument of particular geometry to physically separate two ions of similar masses along their flight trajectories. The mass resolution used here is defined as $m/\Delta m$ [21], where m is the mass of the ion of interest and Δm is the mass difference between its 5 and 95% peak heights. On our instrument the mass resolution equals 9500 for medium and 12,500 for high mass resolution, respectively. For example, the minimum mass resolution to physically separate the flight path of $^{40}Ar^{16}O^+$ (55.957 amu) from that of $^{56}Fe^+$ (55.935 amu) is approximately 2500 (with Δm = 55.957–55.935 amu and m = 55.935 amu). A more detailed description of the ThermoFinnigan Neptune instrument and the high mass resolution measuring technique can be found in Weyer and Schwieters [21]. Sample solutions were nebulised and introduced by the ThermoFinnigan stable introduction system (SIS). This system consists of a combined cyclonic and Scott-type spray chamber. We also assessed the performance of the ESI Apex-Q desolvating apparatus using a low flow (50–100 μL min^{-1}) PFA self-aspirating nebuliser. The ESI Apex-Q apparatus consists of a heated cyclonic glass spray chamber coupled with a Peltier element-cooled glass spiral condenser. Heating of the spray-chamber can be set to 100 or 140 °C and cooling of the condenser to either +2 or −5 °C. An inlet valve allows for N_2 purging to the sample aerosol to further enhance sensitivity and signal stability.

2.1.2. Optimised run conditions

Possible Faraday cup settings for the SSB method, the Cu-doping and two variations of the Ni-doping methods are given in Table 1. The wide focal plane of the Neptune instrument allows simultaneous detection of all Fe isotope ion beams together with $^{52}Cr^+$ and $^{60}Ni^+$ for interference monitoring for the SSB measuring method. Ni-doped Fe measurements may also be made within a single integration cycle, using $^{61}Ni/^{60}Ni$ as instrumental mass bias monitor (Table 1; Ni-doping 1). The $^{62}Ni/^{60}Ni$ ratio as instrumental mass bias monitor is preferable due to its increased mass difference, but requires a dynamic routine (Table 1; Ni-doping 2) with two measurement cycles and correspondingly increased analysis time. A dynamic routine with peak jumping has to be employed for the Cu-doping method as well (Table 1). ^{65}Cu and ^{63}Cu are detected in a first cycle on the Faraday collectors H4 and H2, respectively, while all Fe isotope beams and the interference monitors ^{52}Cr and ^{60}Ni are detected in the second cycle. The total analysis time compared to SSB is doubled, because both cycles are integrated 20 times during 8 s (see Table 2). The magnet is allowed a settling time of 4 s after peak jumping before beam integration is started. While all peaks of cycle 2 are measured on the resolved Fe, Cr, and Ni plateaus, the Cu peaks in cycle 1 are detected full centre.

Table 2
Instrumental parameters for Fe isotope analyses

Parameters	Setting
RF power (W)	1200
Acceleration voltage (V)	−10000
Sampler cone	Ni, 1.1 mm orifice Ø
Skimmer cones	H-type: Ni, 0.8 mm orifice Ø X-type: Ni, oval Ø
Ar gas flow rates (L min^{-1})	
Coolant	15
Auxiliary	0.7–1.0
Nebuliser	1.0–1.15
Analyte matrix	0.3 mol L^{-1} HNO_3
Sample uptake time (s)	80
washout time (s)	100
Cycle integration time (s)	8
Number of cycles per analysis	20

Both HNO_3 and HCl were tested as analyte solutions at molarities ranging from 0.1 to 1 mol L^{-1}. HNO_3 appeared to be superior to HCl, because it yielded a smaller drift of the instrumental mass bias with time as well as better signal stability for Fe. Optimal signal stability and washout times were obtained with a 0.3 mol L^{-1} HNO_3. Interference of $^{40}Ar^{14}N^+$ on $^{54}Fe^+$, which is increased when using HNO_3 as analyte solution, is readily resolved on the ThermoFinnigan Neptune MC-ICP-MS when operating in medium- or high-resolution modes [21]. Stabilising the speciation of Fe in the solutions by adding small amounts of oxidising or reducing agents was also tested but this only resulted in higher instrumental mass bias drift with time.

The principal instrumental parameters that have been investigated during the test runs were radio frequency power (ranging between 1000 and 1300 W), focus lens settings, cycle integration times, overall number of cycles during a single run, various baseline measurements (i.e. on peak zeroes and deflected zeroes or electronic backgrounds) and varying washout times. Optimal run conditions, including sig-

Table 1
Faraday cup settings for different methods of stable Fe isotope ratio determinations on the Neptune MC-ICP-MS

Method		Faraday Cups								
		L4	L3	L2	L1	Center	H1	H2	H3	H4
SSB	Cycle 1	^{52}Cr	–	^{54}Fe	–	^{56}Fe	^{57}Fe	^{58}Fe	–	^{60}Ni
Cu-doping	Cycle 1							^{63}Cu		^{65}Cu
	Cycle 2	^{52}Cr	–	^{54}Fe	–	^{56}Fe	^{57}Fe	^{58}Fe	–	^{60}Ni
Ni-doping 1	Cycle 1	^{53}Cr	–	^{54}Fe	^{56}Fe	^{57}Fe	^{58}Fe	^{60}Ni	–	^{61}Ni
Ni-doping 2	Cycle 1							^{60}Ni	–	^{62}Ni
	Cycle 2	^{52}Cr	–	^{54}Fe	–	^{56}Fe	^{57}Fe	^{58}Fe	–	^{60}Ni

nal and mass bias stability, short washout times, small and reproducible internal run uncertainties and a good external reproducibility of δ^{56}Fe, δ^{57}Fe and δ^{58}Fe values of our in-house JM Fe standard (see Section 2.2), were obtained with the parameters given in Table 2.

2.2. Preparation of Fe standards

Commercially available IRMM-014 Fe was used as the bracketing reference standard, because it is very pure, easily dissolvable and available in large quantities ([26,27]; EU Institute for Reference Materials and Measurements, Geel, Belgium). As internal laboratory standard, a commercially available pure Fe wire (Johnson&Matthey, Fe Puratronic wire, 99.998% purity, lot NM36883; defined here as JM Fe standard) was used for optimising instrumental run conditions and assessing instrumental reproducibility. Differences in Fe isotope composition between our JM Fe and IRMM-014 Fe solutions used here have previously been reported by Walczyk and von Blanckenburg [7] (measured on a Nu-instrument MC-ICP-MS) and Weyer and Schwieters [21] (measured on a ThermoFinnigan Neptune instrument) and thus provide direct inter-laboratory comparison of δ^{56}Fe and δ^{57}Fe values.

JM Fe and IRMM-014 Fe wires were dissolved in 6 mol L^{-1} HCl, followed by dilution in 1 mol L^{-1} HCl to a concentration of approximately 4000 ppm (denoted here as JM Fe and IRMM-014 Fe stock solutions). Measuring solutions of 4–12 ppm were then prepared by drying down small aliquots of these stock solutions, oxidation of Fe in concentrated HNO_3, and after drying down, final dissolution in 0.3 mol L^{-1} HNO_3. For the Cu-doping a commercially available Merck CertiPUR® (1000 ppm Cu in 0.5 mol L^{-1} HNO_3) was used. Small aliquots of this Cu standard were dried down and redissolved in 0.3 mol L^{-1} HNO_3 to yield a concentration of 50 ppm. New Cu standard solutions were prepared for each analysis session.

2.3. Preparation of natural samples

2.3.1. Sample digestion

Silicates were digested in HF–HNO_3; oxides and carbonates were digested in 6 mol L^{-1} HCl. All sample digestions were performed in closed Savillex® PFA containers on a hot plate at 150 °C. Fluoride complexes that formed in silicate samples were destroyed by treating the evaporated samples with concentrated HCl or aqua regia and heating to 170 °C for several hours. Organic samples were digested by microwave agitation in HNO_3–H_2O_2 mixtures. Full oxidation of Fe to its trivalent state was achieved by repeated cycles of dissolution of all samples in concentrated HNO_3, heating to 150 °C and careful drying. All digested samples were then dissolved in 1–2 mL of 6 mol L^{-1} HCl for chromatographic Fe separation.

2.3.2. Fe purification from natural samples

Different Fe separation methods including liquid extraction, precipitation of Fe in various media and anion-exchange chromatography (see also [22]) were tested. Amongst all these methods, chromatographic separation of Fe from its sample matrix was the most reliable in terms of yield, purity of the Fe separates and low Fe blank.

2.3.2.1. Anion-exchange chromatography. Anion-exchange chromatography was performed in a 7.5-mL Spectrum® 104704 polypropylene column using 1 mL of BioRad AG® 1-X8, 100–200 mesh resin. The exchange capacity of 1-mL wet resin is 1.2 mmol $FeCl_4^-$, corresponding to approximately 90 mg Fe. The resin was pre-cleaned with 5 mL of 5 mol L^{-1} HNO_3, followed by 2 mL of H_2O and 5 mL of 0.3 mol L^{-1} HCl. The resin was then pre-conditioned with 4 mL of 6 mol L^{-1} HCl before sample loading. After loading the sample solution onto the resin matrix elements were eluted with 6 mL of 6 mol L^{-1} HCl. Fe was eluted with 2 mL H_2O and 5 mL of 5 mol L^{-1} HNO_3. This HNO_3 step was necessary, because incomplete recovery of Fe can lead to substantial isotope fractionation [19]. It was found that quantitative elution of Fe from the resin with either weak HCl or H_2O required large reagent volumes, while HNO_3 easily breaks down the $FeCl_4^-$ complex and Fe is thus readily stripped from the anion resin. The Fe eluate was then dried down and residual organic substances were oxidised by adding 100 μL concentrated HNO_3. The dried sample Fe was then dissolved in 0.3 mol L^{-1} HNO_3 and diluted to adequate concentrations for matrix check by ICP-OES and isotope ratio determination by mass spectrometry. The separation scheme was calibrated by passing a multi-element ICP standard through the anion chromatography separation and measuring the concentrations of the eluted elements in 1–2 mL steps by ICP-OES. An elution profile is illustrated in Fig. 1. Note that copper, zinc, cadmium and cobalt accompany Fe to some extent. Use of a macroporous resin [16] would accomplish separation of Fe from Cu, but Fe recovery might not be complete. Therefore we prefer the conventional BioRad AG® 1-X8 resin to ensure full Fe elution.

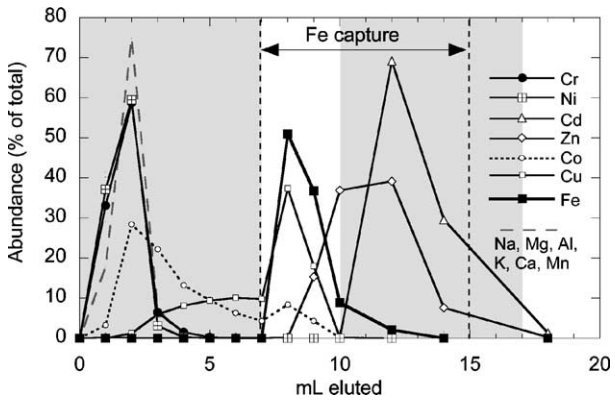

Fig. 1. Elution profile of a synthetic multi-element ICP standard solution through 1 mL of BioRad AG® 1-X8 anion exchange resin. Concentrations were determined by ICP-OES. The black arrow indicates the range in which Fe is collected.

2.3.2.2. Fe precipitation. Fe separates of samples with high transition metal contents or organic matrices may not be entirely matrix-free after anion-exchange chromatography and require further purification. For such samples an additional precipitation step was employed that guaranteed quantitative precipitation of all Fe(III) as Fe(III)OOH while Cu, Zn, Co, Cd, Mn and V as well as organic compounds remained in solution. The sample, dissolved in 0.3 mol L^{-1} HNO_3, was precipitated at pH ≈ 10 with $NH_4(OH)$ (Merck Suprapur®). To ensure full precipitation of Fe, the alkalinised solutions were allowed to equilibrate for 1 h before centrifugation, discarding the supernate solutions and washing the precipitates with pure H_2O. The precipitate was redissolved in HNO_3 for analysis.

3. Results and discussion

3.1. Instrumental reproducibility

3.1.1. Efficiency, molecular interference levels and washout times

Due to decreased entrance slit widths, the ion transmission in medium-resolution mode of the ThermoFinnigan Neptune is reduced approximately eight times as compared to the wider low-resolution slit; the reduction in transmission in high-resolution mode is approximately 16 times. Using the SIS uptake system with a PFA nebuliser and a sample uptake rate of 50–70 μL min^{-1}, total signal intensity for a 1-ppm Fe solution is 3×10^{-11} A in medium-resolution and 1.5×10^{-11} A in high-resolution modes, respectively. These signal intensities corresponds to an ion-to-atom efficiency (i.e. the total amount of Fe ions detected during a measurement compared to the amount of Fe atoms in the measured solution) of our instrument of ∼0.02‰ in medium-resolution and ∼0.01‰ in high-resolution modes. For accurate determination of ^{58}Fe, preferred Fe concentrations are 4–6 ppm for medium-resolution and 10–12 ppm for high-resolution modes. This corresponds to total Fe sample consumptions of 1.5–2.5 and 4–5 μg per analysis, respectively. The Apex-Q system enhances the signal for most elements by 3–6 times, depending on sample uptake. In medium-resolution mode the $^{40}Ar^{16}O^+$ beam of approximately 0.8–1.2 × 10^{-11} A when using the SIS uptake system decreased to between 0.5 and 1.5×10^{-12} A with the Apex-Q uptake system, while the intensity of the Fe signals was increased by a factor of 4–6. The washout behaviour of the ESI Apex-Q apparatus is excellent. It effectively removes a 2.5×10^{-10} A $^{56}Fe^+$ signal to background levels within 80 s and, if operated at ideal conditions, no consecutive sample spikes appear as observed for other desolvating nebulisers. The smallest possible sample size necessary for precise Fe isotope analysis was obtained by using the combination of the ESI Apex-Q apparatus with an X-cone (skimmer). The X-cone is characterised by a different orifice geometry compared to conventional H-cones. It enhances the ion transmission by a factor of about 5, and enables accurate measurements with a Fe concentration of only 125 ppb at medium resolution mode (Table 2). Since sample uptake was 50–70 μL min^{-1} and lasted for approximately 5 min, minimum sample amounts required for precise Fe isotope analyses are approximately 50 ng. However, at such low sample concentrations total Fe beams are much lower than routinely used for data acquisition during this study and higher errors of $\delta^{56}Fe$ and $\delta^{57}Fe$ than reported in this study can be expected, while useful $\delta^{58}Fe$ results are unlikely. Unless indicated otherwise (e.g. in Table 2), the standard set-up for Fe isotope ratio measurements on our instrument during the course of this study was a combination of the SIS uptake system and H-cones.

3.1.2. Fe isotope ratios and instrumental mass discrimination

Fe isotope data measured over an 18 months period under optimised run conditions (Table 2) are plotted in $\ln(^{57}Fe/^{54}Fe)$ versus $\ln(^{56}Fe/^{54}Fe)$ space in Fig. 2. Note that the "natural" composition of IRMM-014 plots in the lower left corner of the diagram, while all our data, both natural and synthetic, yield a much higher abundance of heavy isotopes due to the instrumental mass bias. Furthermore, the range of measured, mass bias-uncorrected isotope compositions exceeds the range of natural Fe isotope fractionations observed by a factor of 2.5. This is due to the variability in instrumental mass discrimination. A $\ln(^{57}Fe/^{54}Fe)$ versus $\ln(^{56}Fe/^{54}Fe)$ diagram can be used to identify the mathematical relationships of this instrumental discrimination. The three commonly used laws (e.g. [28]) plot with slopes of 1.5360 (linear law), 1.5041 (power law) and 1.4881 (exponential law), respectively. Least-square regressions through all synthetic IRMM-014 and JM Fe standard data ($N = 2464$) and through data of natural samples ($N = 862$) yield identical slopes of 1.4894 ± 0.0008 ($R^2 = 0.9998$) and 1.4890 ± 0.0014 ($R^2 = 0.9998$), respectively. Thus, the instrumental mass bias is most accurately described by the exponential law. This has been a general observation for both stable and radiogenic isotope ratio measurements by MC-ICP-MS [29]. However, extrapolating the certified IRMM-014 ratios into the range of measured data using the exponential law reveals that the measured data plot beneath the predicted curve (Fig. 2B). Or, conversely, when the regression line of our data is extrapolated to the natural IRMM-014 values, the line passes beneath the certified value in a three-isotope diagram (Fig. 2C). These offsets can be explained by excess signal on mass 56 through an uncorrected spectral interference, tailing from the $^{40}Ar^{16}O^+$ beam [21], an instrumental mass bias that slightly differs from the exponential law, or a small error on the certified IRMM-014 Fe isotope values, respectively. In $\ln(^{56}Fe/^{54}Fe)$ versus $\ln(^{57}Fe/^{54}Fe)$ space, Arnold et al. [25] obtained a slope for their IRMM-014 values that deviated from the exponential law function. Assuming that their Neptune's mass bias behaviour was best described by the exponential law, these authors modelled that a residual $^{56}FeH^+$ interference on ^{57}Fe of 300 ppm would account for

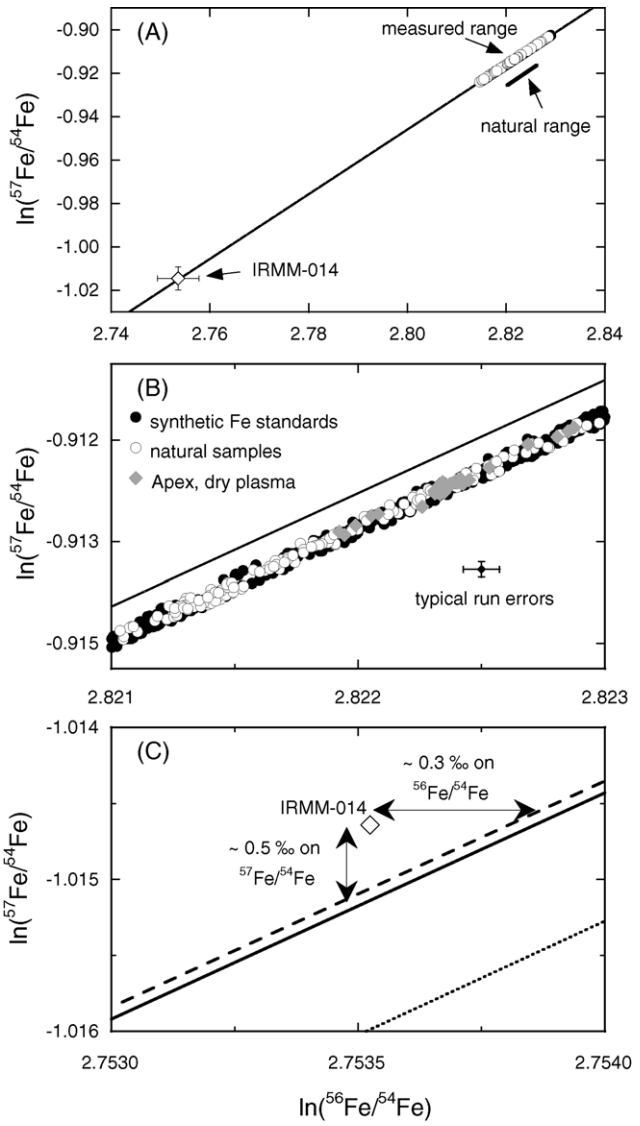

Fig. 2. All Fe isotope data in $\ln(^{57}Fe/^{54}Fe)$ vs. $\ln(^{56}Fe/^{54}Fe)$ space. (A) Open circles are all Fe isotope measurements of synthetic standards and natural samples; open diamond represents the certified iron isotope values of the IRMM-014 standard with uncertainties indicated by the error bars. Note that the least-square regression line through all data extrapolates through the uncertainty limits given for the certified IRMM-014 values; The bold line indicate the range of natural iron isotope variation of approximately 3‰ per AMU. For clarity this line was plotted offset of the fractionation line. (B) Detail of (A) showing that all synthetic and natural samples measured with wet and dry nebulisation plot along a single fractionation line. The solid line is the exponential projection from the certified IRMM-014 values. (C) Detail of (A) with the open diamond representing the certified IRMM-014 value. The solid line is the least-square regression line through all data points; dashed and stippled lines are projections through the average value of our data set with exponential and power law slopes, respectively. The error bars of the IRMM-014 data point exceed the limits of the diagram and are thus not shown.

this deviation. Indeed, these authors measured a $^{56}FeH^+$ interference on ^{57}Fe of 200 ppm in high mass resolution mode on a ThermoFinnigan Element2. However, the data reported here provide no evidence for the presence of a spectral interference like $^{56}FeH^+$. In fact, unresolved interferences of any kind seem unlikely for the following reasons. First, in medium-resolution mode the $^{40}Ar^{16}O^+$ rate decreased from approximately $0.5–1 \times 10^{-11}$ A using wet nebulisation with the SIS uptake system to $0.5–1.5 \times 10^{-12}$ A using dry nebulisation with the Apex-Q system. It is very likely that any residual molecular interference containing oxygen or hydrogen would drop in a similar fashion. However, Fe isotope data that were obtained with both the SIS uptake system (wet plasma) and the Apex-Q system (dry plasma) plot along exactly the same linear array in Fig. 2B. We therefore regard any unresolved $^{56}FeH^+$ interferences on our Fe isotope data of the magnitude described by Arnold et al. [25] as unlikely. Second, we have no evidence for tailing of $^{40}Ar^{16}O^+$ into the $^{56}Fe^+$ beam. Internally correcting all 3326 Fe isotope measurements of our data set using the exponential law and the certified IRMM-014 $^{57}Fe/^{54}Fe$ ratio of 0.362575 yields $^{56}Fe/^{54}Fe = 15.7036 \pm 0.0011$ (2σ). This excellent 2σ reproducibility of 70 ppm on the $^{56}Fe/^{54}Fe$ ratio while the $^{40}Ar^{16}O^+/^{56}Fe^+$ ratios of the different sessions varied by almost two orders of magnitude is strong evidence against any significant tailing. We conclude that the observed offsets in Fig. 2B and C are a combination of the instrumental mass bias not exactly following the exponential law and/or a small error on the certified IRMM-014 values. IRMM-014 was calibrated against a set of synthetic $(n)^{56}Fe/(n)^{54}Fe$ enriched isotope mixtures that were calibrated by metrological weighing upon isotope abundance determination [26,27]. All isotope ratio measurements were performed by thermal ionisation mass spectrometry. Error propagation of the calibration procedure leads to uncertainties in the Fe isotope ratios of several ‰. Thus, the offset between our $^{56}Fe/^{54}Fe$ value and the certified IRMM-014 one at a given $^{57}Fe/^{54}Fe$ ratio of approximately 0.3‰ is well within the calibration uncertainties (Fig. 2C).

3.2. Correction of the instrumental mass bias

3.2.1. Standard-sample bracketing (SSB)

3.2.1.1. Reproducibility of synthetic JM Fe data. The best achievable mass spectrometric reproducibility for $\delta^{56}Fe$, $\delta^{57}Fe$ and $\delta^{58}Fe$ values at the 2σ confidence level under the optimised running conditions (Table 2) are presented in Table 3 and Fig. 3. The excellent agreement of $\delta^{56}Fe$, $\delta^{57}Fe$ and $\delta^{58}Fe$ values for JM Fe using wet (SIS) and dry (Apex-Q) sample uptake, and while operating the Neptune at both medium- and high-mass resolution modes, gives us confidence that all poly-atomic interferences are well-resolved for all tested instrumental set-ups. The Fe isotope composition of JM Fe obtained during this study agrees very well with those reported in Walczyk and von Blanckenburg [7] and Weyer and Schwieters [21].

All $\delta^{56}Fe$ values follow a Gaussian distribution (Fig. 3B). The observation that the JM Fe data plot along the calculated, theoretical fractionation line in $\delta^{57}Fe$ versus $\delta^{56}Fe$ space of Fig. 3A reveals that the mass-dependent scatter of data points is unlikely to be due to unresolved interferences

Table 3
External reproducibility for JM Fe standard measurements using different instrumental settings

Instrumental parameters	Conc. solution (ppm)	^{56}Fe (V)[a]	δ^{56}Fe (‰)	2 S.D.	δ^{57}Fe (‰)	2 S.D.	δ^{58}Fe (‰)	2 S.D.	No. of runs
Measured January–August 2003									
SIS, medium resolution, H-cones	6	16–25	0.424	0.039	0.622	0.063	0.85	0.31	127
SIS, high resolution, H-cones	12	16–25	0.421	0.046	0.626	0.075	0.84	0.49	104
		Average	0.423	0.042	0.624	0.069	0.84	0.40	231
Apex, medium resolution, H-cones	2	22–30	0.424	0.044	0.624	0.081	0.82	0.31	44
Apex, high resolution, H-cones	4	22–30	0.420	0.050	0.621	0.080	0.76	0.45	88
Apex, medium resolution, X-cones	0.25	15	0.422	0.023	0.619	0.047	0.68	0.44	5
Apex, medium resolution, X-cones	0.125	∼7	0.400	0.058	0.610	0.114	0.37	0.80	5
		Average	0.422	0.048	0.622	0.080	0.78	0.41	142
Measured August 2003–August 2004									
Variable settings	6–12	16–30	0.423	0.049	0.625	0.073	0.83	0.41	268
		Grand average	0.423	0.046	0.624	0.073	0.83	0.41	641
Walczyk and von Blanckenburg [7]			0.460	0.200	0.680	0.300	–	–	
Weyer and Schwieters [21]			0.350	0.140	0.540	0.160	–	–	

[a] Measured with a 10^{11} Ohm resistor.

or an over-correction of the $^{54}Cr^+$ interference correction on $^{54}Fe^+$. The latter can be concluded since JM Fe and IRMM-014 Fe are high-purity materials, virtually free of Cr. It is also unlikely that memory build-up in the uptake system or on the cones causes the shift in δ^{57}Fe and δ^{56}Fe values of repeated measurements of a particular sample (here JM Fe standard) along the mass-dependent fractionation line, because the same effect can be observed when measuring IRMM-014 Fe as samples and bracketing standards. Accurate determination of δ^{58}Fe values requires minimum signal intensities on the $^{58}Fe^+$ beam of 0.6×10^{-12} A, corresponding to $^{56}Fe^+$ beams of approximately 2.0×10^{-10} A. If only JM Fe data that were assessed at such intensity levels are taken into account the 2σ reproducibility on the δ^{58}Fe value decreases from 0.41‰ (Table 3) to 0.28‰.

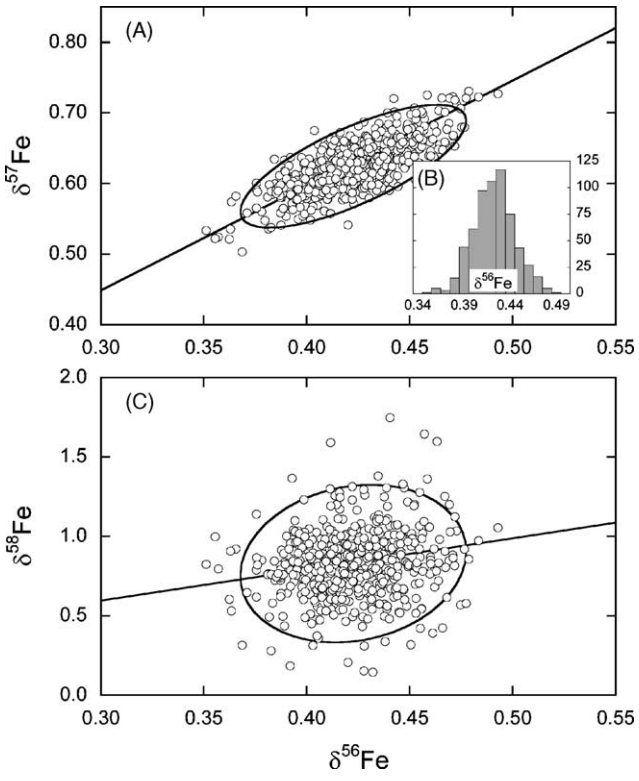

Fig. 3. Mass spectrometric reproducibility. (A) Open circles are 641 single JM Fe data points measured against IRMM-014 Fe over the course of 18 months plotted in a δ^{57}Fe vs. δ^{56}Fe diagram. Dotted squares are the averages of measuring sequences of JM data analysed under optimised run conditions. Error ellipse indicates the 95% confidence for JM Fe data measured under optimised run conditions. (B) Histogram of δ^{56}Fe values for JM Fe measured under optimised run conditions. (C) δ^{58}Fe vs. δ^{56}Fe diagram for JM Fe data. Symbols are the same as for (A).

A statistical assessment of the external instrumental reproducibility in δ^{57}Fe versus δ^{56}Fe and δ^{58}Fe versus δ^{56}Fe spaces was performed by a means of correlated error ellipses [30,31], rather than simply reporting standard deviation bars for individual data points. For this purpose, the error ellipses illustrated in Fig. 3A and C were assessed by a chi-squared statistical test for two degrees of freedom at a 5% level of risk [30–32]. The error correlation of the JM Fe data in the δ^{57}Fe versus δ^{56}Fe diagram is 0.697, while that in the δ^{58}Fe versus δ^{56}Fe space is only 0.035. The high degree of correlation between δ^{57}Fe and δ^{56}Fe suggests that count-statistical errors are not the limit of reproducibility for both these ratios. Although not supported by hard evidence, we assume that the most likely source of scatter is introduced by the inaccuracy of the instrumental mass bias correction. The low correlation between δ^{58}Fe and δ^{56}Fe most likely reflects the higher uncertainty on the δ^{58}Fe values caused by poor counting statistics on the small $^{58}Fe^+$ beams and the significant $^{58}Ni^+$ interference correction on $^{58}Fe^+$. Precision of the δ^{58}Fe value might be increased by using aluminium or platinum rather than standard Ni cones, which are the source of most of the small ($<1 \times 10^{-14}$ A levels) Ni beams that slightly diminish the accuracy of δ^{58}Fe values.

3.2.1.2. Intensity matching. Weyer and Schwieters [21] reported a 50-ppm contribution of the $^{40}Ar^{16}O^+$ tail to the $^{56}Fe^+$ peak in medium-mass resolution mode. Such a contribution was not observed for our measurements (see Section 3.1.2);

furthermore, such a tailing of $^{40}Ar^{16}O^{+}$ would be cancelled out by the bracketing procedure. If tailing is present, however, it might affect the accuracy of samples $\delta^{56}Fe$ values, if the samples concentrations were poorly matched to those of the bracketing standard. In addition, Malinovsky et al. [23] observed a correlation between the concentration of Fe analyte solutions and instrumental mass bias. Such an effect also might cause inaccurate stable Fe isotope determinations for samples whose concentrations were poorly matched to those of their bracketing IRMM-014 Fe standard. Therefore a series of measurements was carried out where the concentrations of JM Fe solutions were varied between 0.5 and 1.5 times that of their IRMM-014 Fe bracketing solution. This experiment was carried out at two different intensity levels; once with IRMM-014 Fe at 1.5×10^{-10} A and once with IRMM-014 at 2.5×10^{-10} A intensity. Neither of the two sets of data (Fig. 4) reveals significant influence on the accuracy of the Fe isotope composition of JM Fe. Nevertheless, we routinely determine Fe concentrations of natural samples by flame AAS or optical ICP prior to isotope analysis and match concentrations to within 10% of the concentration of the bracketing IRMM-014 Fe solution.

3.2.1.3. Correction of the interfering isotopes $^{54}Cr^{+}$ on $^{54}Fe^{+}$ and $^{58}Ni^{+}$ on $^{58}Fe^{+}$. An accurate ^{54}Cr correction on ^{54}Fe is essential, because it is common practise to use ^{54}Fe as normalising isotope for reporting Fe isotope ratios. Our approach has been to adopt a separation procedure that removes Cr from Fe quantitatively. Nevertheless, it is important to evaluate the correction of ^{54}Cr on ^{54}Fe, because uncertainties in this correction are not easily revealed in $\delta^{57}Fe$ versus $\delta^{56}Fe$ plots. The shift of a data point caused by under- or over-correction of ^{54}Cr plots along a vector with a slope of 1 in such a diagram, while the natural or exponential fractionation line has a slope of 1.4881. Assuming that a measurement was not accurately corrected for a ^{54}Cr interference, the data point may shift along the chromium vector with a slope of 1 over a range of ± 0.1 $\delta^{56}Fe$, while its error ellipse still overlaps the natural fractionation line. However, removal of Cr from Fe by the anion chromatographic separation outlined above and illustrated in Fig. 1 is quantitative and for most samples the $^{54}Cr/^{54}Fe$ ratio is much less than 0.025‰.

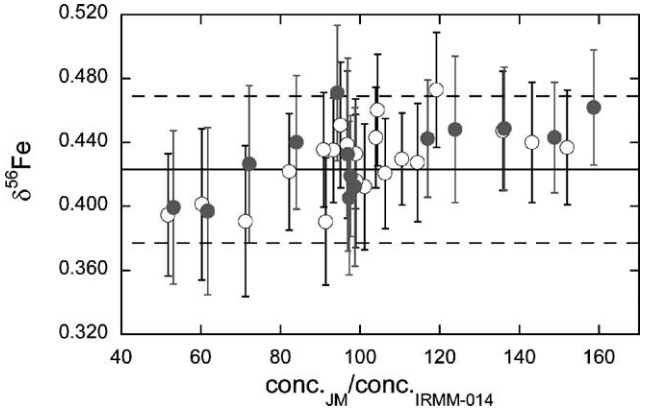

Fig. 4. Effects of signal matching between standards and samples. $\delta^{56}Fe$ values for JM Fe standard measurements with variable JM concentrations were bracketed with an IRMM-014 Fe standard solution of constant concentration. The experiment was performed at IRMM-014 Fe intensities of 1.5×10^{-10} A (grey circles) and at 2.5×10^{-10} A (open circles). Solid lines give the average of JM Fe $\delta^{56}Fe$ and $\delta^{57}Fe$ values (Table 3) and the dashed lines its 2σ confidence intervals.

Successful interference corrections must take into account that the instrumental mass bias affects not only the relative abundances of the Fe isotopes, but those of Cr and Ni too. Thus, the $^{52}Cr/^{54}Cr$ and $^{60}Ni/^{58}Ni$ ratios of assumed "common" compositions must be artificially fractionated before subtracting ^{54}Cr and ^{58}Ni intensities from measured beam intensities on masses 54 and 58, respectively. We calculate the mass bias of Ni and Cr from the mass bias of the measured $^{57}Fe/^{56}Fe$ ratio of samples relative to the certified IRMM-014 value. However, three minor errors are included in this correction mode: (1) the assumption that Cr, Ni and Fe share the same mass bias may be flawed [16,33]. (2) The stable $^{57}Fe/^{56}Fe$ ratio of samples differ from that of IRMM-014 by up to ± 1.5‰. (3) The stable $^{52}Cr/^{54}Cr$ and $^{60}Ni/^{58}Ni$ ratios of the samples might also be fractionated. However, these error sources are almost negligible compared to the ~7% instrumental fractionation on the $^{52}Cr/^{54}Cr$ and $^{60}Ni/^{58}Ni$ ratios. The accuracy of the $^{54}Cr^{+}$ interference correction on $^{54}Fe^{+}$ as well as the $^{58}Ni^{+}$ interference correction on $^{58}Fe^{+}$ were tested by doping JM Fe standards with varying amounts of Cr and Ni. Results of the experiment are illustrated in Fig. 5. No bias on $\delta^{56}Fe$ was introduced by an inaccuracy in Cr interference correction up to a $^{54}Cr/^{54}Fe$ level of 1‰. $\delta^{58}Fe$ appeared to be unaffected up to $^{58}Ni/^{58}Fe$ of 1%. Nevertheless, Fe isotope analyses with $^{54}Cr/^{54}Fe > 0.1$‰ are rejected from data sets, while $\delta^{58}Fe$ values of samples with $^{58}Ni/^{58}Fe > 1$% are considered unreliable.

3.2.1.4. Matrix effects. Even small differences in the matrix of the Fe analyte solution of natural samples might influence the instrumental mass bias [14,16,20,33]. Such matrix effects might be introduced by elements that were not fully removed from Fe during chemical separation, organic substances, the speciation of the Fe, or differences of the solution acid strength relative to that of the standard. Matrix effects can potentially shift the Fe isotope composition of samples along the natural fractionation line. However, they might not necessarily be discovered since the effects can reproduce during mass spectrometric and chemical duplication. Although the true nature of such matrix effects on the instrumental mass bias is still poorly understood, elimination of such effects is crucial for the accuracy of data. Fig. 1 indicates that small amounts of Cu, Zn, Cd and Co might be released together with Fe from the anion resin. Concentrations of Co and Cd in natural materials occur at trace amounts only and are thus not likely to significantly affect the instrumental mass bias. However, Cu and Zn in Fe separates might reach concentration levels that potentially affect accurate stable Fe isotope determinations. This is of particular concern when measur-

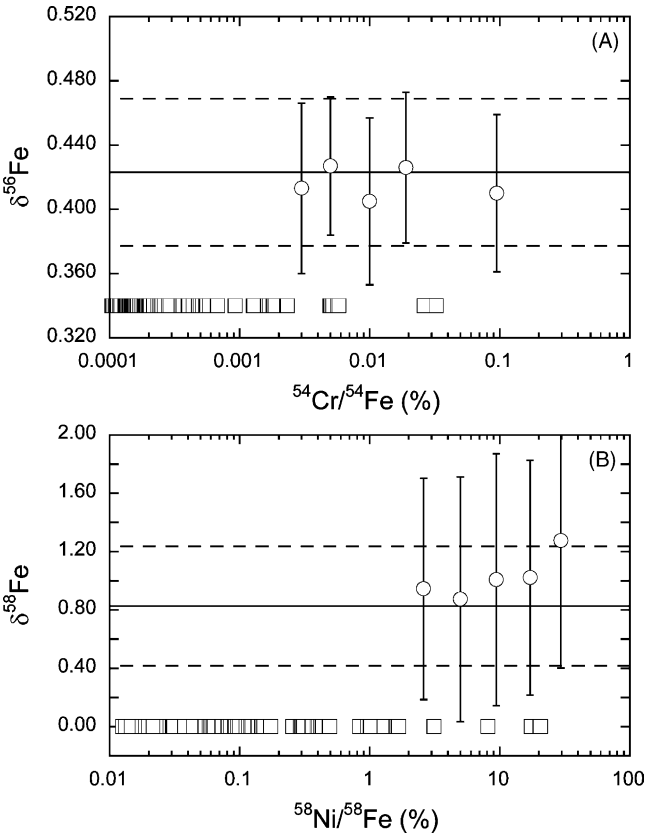

Fig. 5. Accuracy tests for interference corrections of ^{54}Cr on ^{54}Fe and ^{58}Ni on ^{58}Fe (open circles). (A) δ^{56}Fe values for JM Fe measured against IRMM-014 and doped with varying amounts of Cr. Open squares give the measured ^{54}Cr/^{54}Fe ratios of all natural samples that were measured during the course of this study. The ^{54}Cr/^{54}Fe ratios of natural samples after Fe purification are usually smaller than 0.0025%. (B) δ^{58}Fe values for JM Fe measured against IRMM-014 Fe and doped with varying amounts of Ni. Open squares give the measured ^{58}Ni/^{58}Fe ratios of all natural samples measured during the course of this study. The ^{58}Ni/^{58}Fe ratios of natural samples are usually smaller than 1%. In both graphs the solid lines give the average of δ^{56}Fe and δ^{58}Fe of JM Fe (Table 3), respectively, and the dashed line indicate their 2σ confidence intervals.

ing ore samples and sulphides. Consequently, the influence of Cu, Zn, Cd and Co on the instrumental mass bias and thus on the accuracy of Fe isotope data was tested. This was done by doping JM Fe standards with different amounts of these elements. Fig. 6 reveals no influence of Cu, Zn, Cd and Co on the δ^{56}Fe and δ^{57}Fe values of JM Fe. Whether the larger scatter of JM's δ^{56}Fe and δ^{57}Fe values observed for $c_{Cu,Zn,Co,Cd}/c_{Fe}$ ratios of >10% is due to a matrix effect is hard to evaluate, since the data are still within the external reproducibility of JM's Fe isotope composition. In our laboratory, the amounts of residual Cu, Zn, Cd, and Co in the Fe analyte solution are determined amongst other trace and major elements by ICP-OES. In this context, it is important to bear in mind that if instrumental mass bias is corrected by doping of Fe samples with Cu [20,25] or Ni [22,23], those elements and all their elemental isobars from the samples during anion exchange and Fe(III)OOH precipitation.

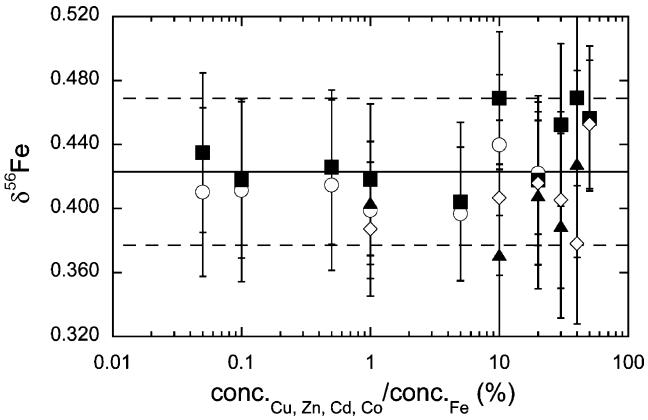

Fig. 6. Effect of elements left in the Fe fraction after chemical processing on isotope measurements. δ^{56}Fe (A) and δ^{57}Fe (B) values for JM Fe measured against IRMM-014 Fe-doped with different amounts of Cu (open circles), Zn (filled squares), Cd (open diamonds) and Co (filled triangles). Solid line gives the average of JM Fe δ^{56}Fe value (Table 3) and the dashed lines its 2σ confidence intervals.

To assess the potential mass bias introduced by different natural sample matrices, the samples' Fe was separated from its matrix by the anion exchange procedure outlined above. JM Fe standard (usually 20–50% of the sample's original amount of Fe) of known isotope composition was added to the now Fe-free matrices and homogenised by repeated drying down and uptake in concentrated HNO_3. The JM Fe was then separated from the sample matrices by the chemical separation procedure described above and measured for its stable Fe isotope composition. We regard such tests of natural matrices as more genuine than simply adding extraneous elements as matrix [14] or experiments as shown in Fig. 6. Fe data of these tests are described as "matrix test" in Table S1 of *the supporting online material* to this publication. The extensive set of matrix tests performed on silicate rocks, oxides and carbonates reveal excellent agreement with JM Fe isotope composition given in Table 2. There was one exception, however. Matrix tests of a first column pass of a set of beef liver samples (1st column pass, *supporting online material* Table S1) reproducibly exhibited slightly lower δ^{56}Fe (by 0.03–0.07‰) and δ^{57}Fe (by 0.06–0.1‰) values than those for matrix-free JM Fe. Although this small bias was within limits of the overall reproducibility, we investigated its source by passing the respective Fe separates a second time through the anion exchange columns. This time Fe isotopes identical to matrix-free JM Fe were measured (Table S1). We infer that during analyses of the liver samples after a single column pass a small matrix effect might have generated a minor shift in instrumental mass bias. Although all of these results are within error limits, we would like to draw attention to two important points. First, good reproducibility of the Fe isotope composition of chemical replicates of natural samples might not reliably prove the absence of matrix effects. Second, certain samples, in particular those with organic-rich matrices, need to be subject to multiple passes over the anion exchange columns or to a

combination of anion exchange and Fe(III)OOH precipitation.

3.2.1.5. Reproducibility of natural samples. The reproducibility of stable Fe isotope determinations were tested on a variety of natural samples with different matrices. Samples with inorganic matrices were silicate rocks, oxides (magnetite, ilmenite, hematite) and carbonates, while organic matrices included liver, muscle tissue and blood (Table 4). When accounting for the instrumental mass bias with the standard-sample bracketing method, it is essential to investigate two different reproducibility levels for natural samples: (1) the mass spectrometrical reproducibility, determined by replicate measurements of the same analyte solution of natural samples and (2) the chemical reproducibility, determined by measuring aliquots of the same sample digest that were passed separately through different anion-exchange columns. The reproducibility of a data set consisting of different samples with a variety of Fe isotope compositions can be determined with following equation:

$$\sigma_x = \sqrt{\frac{\sum_{i,j=1}^{n,m}(x_i - \bar{x}_j)^2}{\sum(n_{i,j} - 1)}} \quad (2)$$

where $x_{i,j}$ denotes either δ^{56}Fe, δ^{57}Fe or δ^{58}Fe values of the replicate measurement i (1–n) of sample j (1–m), $x_{j-\mathrm{mean}}$ gives the average of all replicate measurements of sample j, and $n_{i,j}$ gives the number of measured replicates i of sample j. For the calculation of the reproducibility of the chemical replicates i of a certain natural sample j with Eq. (2), $x_{i,j}$ was chosen to be the average of all mass spectrometric replicates of i. The reproducibilities of a comprehensive data set of natural samples can be found in Table S1 of the *supporting online material*. The two principal results are: First, the reproducibilities of the stable Fe isotope composition of chemical replicates of individual natural samples are identical to the mass spectrometric reproducibilities of the same samples. Second, the external reproducibilities of δ^{56}Fe, δ^{57}Fe and δ^{58}Fe values of mass spectrometric and chemical replicates of all natural samples at the 2σ level (Table 4) as calculated from 318 measurements of 95 samples (those in Tables 4 and 5) from Eq. (2) are only slightly (if at all) inferior to the instrumental reproducibility (the latter was determined on the synthetic JM Fe standard; Table 3).

The excellent agreement of δ^{56}Fe, δ^{57}Fe and δ^{58}Fe reproducibilities between chemical replicates of natural samples with different matrices (Table 4) allows for an assessment of an overall external reproducibility. Mass spectrometric and chemical replicates of a total of 318 Fe isotope measurements of silicate rocks, oxides, carbonates, livers, muscle tissue and blood are plotted in Fig. 7A and B by normalising each individual measurement of a sample to either its average of mass spectrometric replicates or, where available, to the average of chemical replicates of that specific sample. The 95% confidence levels for the δ^{56}Fe, δ^{57}Fe and δ^{58}Fe values are 0.049, 0.071 and 0.28‰, respectively. The error correlation of the data in δ^{57}Fe versus δ^{56}Fe space is 0.831 and that in δ^{58}Fe versus δ^{56}Fe space is 0.315, respectively. The 95% confidence error ellipses illustrated in Fig. 7 were calculated using chi-squared statistics of the data set [30,31].

3.2.2. Cu-doping and comparison to SSB

The accuracy of the SSB method for stable Fe isotope determinations has recently been questioned [25], especially when separating the iron of a sample from its matrix with a single anion chromatography step. Arnold et al. [25] employed a measuring technique involving addition of Cu of known isotope composition to Fe standards and samples for internal instrumental mass bias correction. Since these authors also alternated measurements of Fe standards and Fe samples, they were able to directly compare external mass bias correction using SSB with internal correction using Cu. They determined that the reproducibilities of δ^{56}Fe values of natural samples were inferior for the SSB compared to the Cu-doping method. Arnold et al. [25] attributed this observation to mass bias effects caused by residual, unseparated matrix in the Fe analyte solutions of the samples. In our approach, however, a single anion exchange column pass of most inorganic and even organic samples yielded pure Fe separates with no residual, unseparated matrix. The reproducibilities in δ^{56}Fe values of these samples using SSB were virtually identical to those of synthetic Fe standards (Fig. 7, Table 4)

Table 4
External reproducibilities of mass spectrometric and chemical replicates of inorganic and organic samples

	Replicate measurements					Chemical replicates				
	Samples	Runs	2σ δ^{56}Fe (‰)	2σ δ^{57}Fe (‰)	2σ δ^{58}Fe (‰)	Samples	Runs	2σ δ^{56}Fe (‰)	2σ δ^{57}Fe (‰)	2σ δ^{58}Fe (‰)
Inorganic matrices										
Silicates	11	45	0.031	0.049	0.33	14	38	0.019	0.032	0.26
Oxides	16	54	0.055	0.088	0.22	7	20	0.053	0.078	0.22
Carbonates	2	23	0.051	0.084	0.26	4	12	0.036	0.033	0.23
Average	29	122	0.050	0.079	0.28	25	70	0.043	0.064	0.25
Organic matrices										
Liver	11	50	0.064	0.102	0.23	2	9	0.035	0.038	0.18
Muscle	6	13	0.061	0.076	0.28	–	–	–	–	–
Blood	43	109	0.064	0.081	0.25	4	8	0.055	0.088	0.18
Average	60	172	0.064	0.088	0.24	6	17	0.043	0.060	0.18

Table 5
Comparison of SSB and Cu-doping reproducibilities

	SSB-only			Cu-doping		
	δ^{56}Fe (‰)	δ^{57}Fe (‰)	δ^{58}Fe (‰)	δ^{56}Fe (‰)	δ^{57}Fe (‰)	δ^{58}Fe (‰)
All sessions combined (# of runs = 115)						
Average	0.428	0.632	0.81	0.424	0.626	0.80
2σ	0.055	0.092	0.58	0.042	0.071	0.52
Cu-doping session measured during warm-up of the Neptune						
JM-01	0.399	0.591	0.83	0.418	0.620	0.87
JM-02	0.059	0.076	0.00	0.396	0.578	0.67
JM-03	0.493	0.727	1.05	0.461	0.680	0.99
JM-04	0.430	0.616	0.65	0.424	0.606	0.64
JM-05	0.407	0.601	0.53	0.423	0.625	0.56
JM-06	0.439	0.669	0.15	0.403	0.615	0.45
JM-07	0.369	0.503	0.31	0.426	0.588	0.43
JM-08	0.434	0.643	0.93	0.428	0.635	0.92
JM-09	0.339	0.490	0.35	0.378	0.549	0.42
JM-10	0.475	0.706	0.57	0.462	0.686	0.54
JM-11	0.467	0.657	0.80	0.452	0.681	0.83
JM-12	0.455	0.669	0.42	0.471	0.693	0.45
Average	0.397	0.579	0.55	0.428	0.630	0.65
2σ	0.231	0.348	0.64	0.057	0.094	0.41

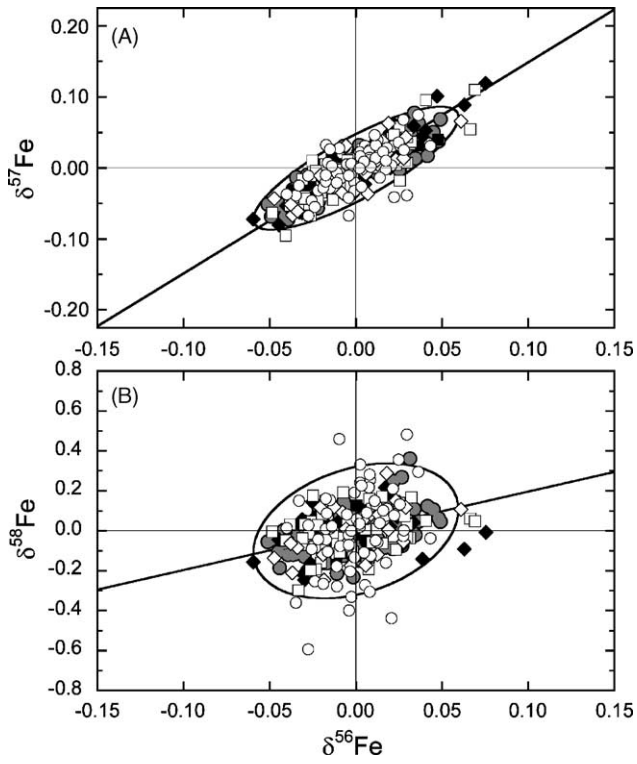

Fig. 7. Error correlation of natural samples. (A) Fe isotope data of silicate rocks (open circles), carbonates (open diamonds), oxides (open squares), livers (filled diamonds), muscle tissue (filled squares) and blood (filled circles) in a δ^{57}Fe vs. δ^{56}Fe diagram. The Fe isotope composition of single measurements of a sample were normalised to either the average of the respective samples' mass spectrometric replicates or, where possible, to the average of the respective samples chemical replicates. (B) Fe isotope data of the same data set as for (A) plotted in a δ^{58}Fe vs. δ^{56}Fe diagram. Symbols in (B) are the same as in (A) and the solid lines are the natural fractionation lines. Parameters for calculation of the 95% confidence error ellipses are given in the text.

and equal to those reported by Arnold et al. [25] using the Cu-doping method. To further evaluate the two approaches a Cu-doping method was set up on the Neptune instrument at Hannover.

Instrumental mass bias correction by the Cu-doping method was investigated over the course of 3 months. A known difficulty of ICP doping techniques is that element pairs usually are not subjected to the same instrumental mass bias. This effect, which is caused by the space-charge effect in the plasma and interface region of ICP instruments has been extensively described in the literature [16,19,20,25,28]. We addressed the differential fractionation behaviour of Cu and Fe by performing a Cu-doped bracketing technique [25] in which Cu-doped samples were measured alternatingly with Cu-doped IRMM-014 standards (here defined as Cu-doped analytical sessions). The mass bias-corrected Fe isotope composition of a sample was then expressed relative to the average Fe isotope composition of the directly preceding and following IRMM-014 standards. Throughout all sessions an assumed ^{65}Cu/^{63}Cu ratio of 0.44513 and an exponential fractionation law were applied for instrumental mass bias correction (see [25]).

3.2.2.1. Reproducibility of JM Fe standard data. Fe isotope ratios of a sample measured during a Cu-doped analytical session have been compared after correcting by both the SSB-only, ignoring the Cu correction made in the same run, and the Cu-doping method. Doing this, excellent agreement between results from both approaches is obtained for the JM Fe measurements (Table 5). These JM Fe data are also identical to those that were obtained with the pure SSB method for mass bias correction (Table 3). Interestingly, Cu-doped δ-values are subject to the same error correlation as that observed for pure SSB, when plotted in a δ^{57}Fe versus δ^{56}Fe diagram

(Fig. 3). Again we assume that this mass-dependent correlation of δ^{56}Fe and δ^{57}Fe values is due to minor shifts in the instrumental mass discrimination that were not fully removed with the Cu correction. In this regard Cu-doping presents no improvement over SSB. Reproducibilities of the SSB-only corrected δ^{56}Fe, δ^{57}Fe and δ^{58}Fe values given in Table 5 are slightly inferior to those obtained by Cu-free SBB (Table 3). This can be explained by the fact that optimised run conditions used for the SSB method described in Section 2.1.2 are not achieved for SSB-only corrected data obtained during Cu-doped analytical sessions: time intervals between Fe measurements are doubled, resulting in a less tight bracketing sequence. This enhances the effect of non-linear instrumental drift on the linear interpolation of the data. A true advantage of the Cu-doping method over SSB is illustrated in Fig. 8 and Table 5. The mass bias drift of the Neptune MC-ICP-MS tends to be high and unstable for the first 2 h after igniting the plasma and for approximately 30 min after changing instrumental parameters (sample gas flow, torch position and lens settings). Measuring stable iron isotope compositions under such conditions using the SSB method for instrumental mass bias correction may lead to inaccurate analyses, as

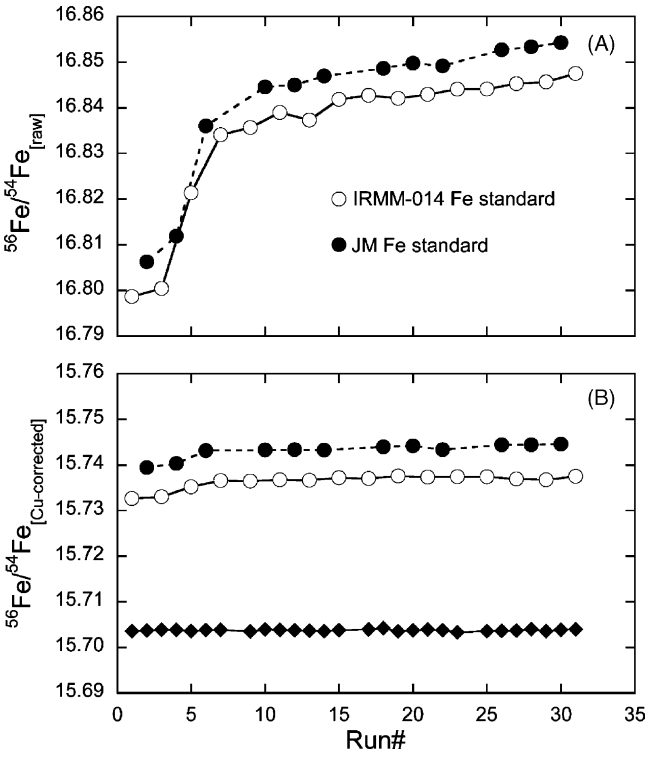

Fig. 8. (A) Mass bias uncorrected ^{56}Fe/^{54}Fe values of alternating measurements of the IRMM-014 and JM Fe standards. Note that the *x*-axis is equal to a time axis. The difference between JM and adjacent IRMM standards directly translates into the δ^{56}Fe values of the JM measurements. (B) The same data for IRMM-014 and JM standards as in (A), but this time the ^{56}Fe/^{54}Fe values were mass bias-corrected using the Cu-doping method. The grey diamonds are the internally corrected ^{56}Fe/^{54}Fe values using the certified IRMM-014 ^{57}Fe/^{54}Fe value of 0.362575 and an exponential law, illustrating superior reproducibility of internally corrected data compared to those corrected externally using Cu.

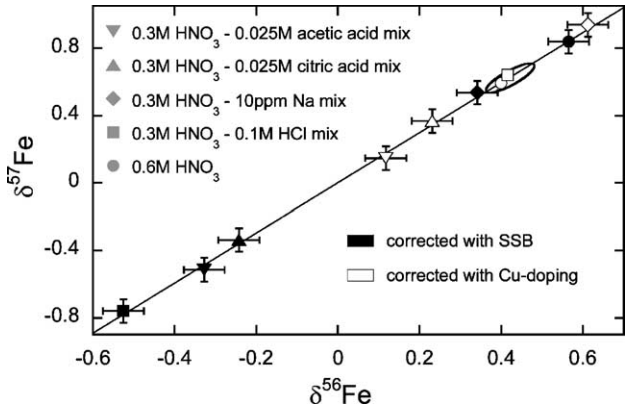

Fig. 9. Measured iron isotope composition in δ^{57}Fe vs. δ^{56}Fe space of JM Fe standards that were doped with different artificial matrices, using SSB-only (filled symbols) and Cu-doping (open symbols) to account for instrumental mass bias. Solid line gives the exponential fractionation line and the error ellipse indicates the 95% uncertainty interval of the JM Fe isotope composition in 0.3 mol L^{-1} HNO_3 as measured both by SSB and Cu-doping methods.

demonstrated by the second JM data point in Fig. 8A and Table 5. The same JM measurement corrected with the Cu-doping method yields, within uncertainties, accurate δ^{56}Fe, δ^{57}Fe and δ^{58}Fe values (see Table 5).

3.2.2.2. Matrix effects. Simple comparison of the SSB with the Cu-doping method was carried out by doping JM Fe standards with different inorganic and organic matrices (Fig. 9). The addition of 0.1 mol L^{-1} HCl leads to the largest (−1‰) shift in the δ^{56}Fe value with the SSB-only method. The δ^{56}Fe value of that JM that was taken up in 0.6 mol L^{-1} HNO_3 instead of 0.3 mol L^{-1} HNO_3 was offset by approximately +0.12‰. Both of these JM measurements yield accurate δ^{56}Fe and δ^{57}Fe values when instrumental mass bias is corrected by the Cu-doping method. However, Cu-doping did not fully correct standards with artificial organic matrices. Although the Cu-doping corrected δ^{56}Fe and δ^{57}Fe values for

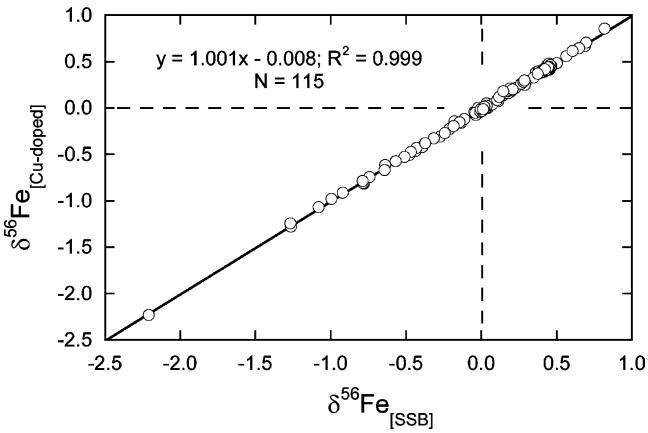

Fig. 10. Comparison of δ^{56}Fe values of natural samples measured during Cu-doped analytical session corrected for instrumental mass bias with SSB-only (*x*-axis) and Cu-doping (*y*-axis) methods. The sample set includes silicate rocks and minerals, meteorites, carbonates, oxides and sulphides.

the citric and acetic acid mixes are closer to the true JM Fe isotope composition than the values obtained by SSB-only correction, they are still well outside its 2σ reproducibility limits given by the error envelope in Fig. 9. Adding 10 ppm sodium to the JM Fe standard solution affected the mass bias such that its SSB-only δ^{56}Fe was slightly too low. However, the effect of sodium on Cu-corrected δ^{56}Fe is much larger, with δ^{56}Fe and δ^{57}Fe values of this JM Fe standard being far too high. Scans on the Cu masses revealed that there is a slight spectral interference on mass 63 that correlates with the Na content in the analyte solution. This interference is most likely $^{40}Ar^{23}Na^{+}$ that leads to underestimation of the Cu mass bias and thus to inadequate correction of the sample Fe isotope ratios.

Table 6
δ^{56}Fe values for different mass bias correction methods

Purification	SSB session (δ^{56}Fe)	Cu-doping session	
		δ^{56}Fe SSB-only	δ^{56}Fe Cu-doping
Fe–Mn nodule 1			
1CP	−0.417	−0.411	−0.349
	−0.471	–	–
	−0.411	–	–
	−0.435	–	–
2CP	−0.437	−0.457	−0.380
1C&P	−0.467	−0.476	−0.455
Average	−0.440	−0.448	−0.395
2σ	0.050	0.067	0.109
Fe–Mn nodule 2			
1CP	−0.244	−0.238	−0.161
	−0.219	–	–
	−0.215	–	–
2CP	−0.249	−0.277	−0.122
1C&P	−0.303	−0.281	−0.276
Average	−0.246	−0.265	−0.186
2σ	0.070	0.048	0.160
Fe–Mn nodule 3			
1CP	−0.403	−0.394	−0.372
	−0.340	–	–
	−0.327	–	–
2CP	−0.364	−0.352	−0.354
1C&P	−0.344	−0.384	−0.356
Average	−0.356	−0.377	−0.361
2σ	0.059	0.043	0.019
Fe–Mn module 4			
1CP	−0.320	−0.382	−0.296
	−0.360	–	–
	−0.308	–	–
2CP	−0.285	−0.320	−0.318
1C&P	−0.348	−0.352	−0.384
Average	−0.324	−0.351	−0.332
2σ	0.061	0.062	0.092
Fe–Mn module 5			
1CP	−0.376	−0.402	−0.399
	−0.354	–	–
	−0.366	–	–
2CP	−0.375	−0.415	−0.391
1C&P	−0.388	−0.446	−0.381
Average	−0.372	−0.421	−0.390
2σ	0.025	0.045	0.018
Fe–Mn module 6			
1CP	−0.431	−0.459	−0.452
	−0.389	–	–
	−0.424	–	–
2CP	−0.420	−0.466	−0.486
1C&P	−0.428	−0.461	−0.389
Average	−0.418	−0.462	−0.442
2σ	0.034	0.008	0.099

1CP: 1 × anion exchange. 2CP: 2 × anion exchange. 1CP&P: 1 × anion exchange plus $NH_4(OH)$ precipitation.

3.2.2.3. Reproducibility of natural samples. During the course of this study 115 natural samples with different matrices have been determined during Cu-doped analytical sessions. Fig. 10 illustrates excellent agreement between δ^{56}Fe values that were corrected for instrumental mass bias by the SSB method and those that were corrected with the Cu-doping method. The Fe of most of these samples was extracted by a single anion exchange chromatography step. There were some exceptions from the exact agreement between SSB and Cu-doping corrected data, however, that are explored in some more detail. Samples with high transition metal contents, such as diagenetic Fe–Mn nodules, still preserved Cu/Fe and Zn/Fe concentration ratios of approximately 0.2 after Fe purification (see Section 2.3.2). Such high transition metal contents might affect the mass bias of Fe isotope measurements, and thus lead to inaccurate δ^{56}Fe, δ^{57}Fe and δ^{58}Fe values when applying SSB for mass bias correction. The high natural Cu content left in the Fe analyte solutions of Fe–Mn nodules after repeated anion exchange column passes, on the other hand, might add Cu of a ^{65}Cu/^{63}Cu ratio that is different from the standard Cu used for the doping. This natural Cu is likely to be fractionated by partial release from the anion exchange resin [16]. In this case, Cu-doping might lead to inaccurate δ^{56}Fe, δ^{57}Fe and δ^{58}Fe values. For the Fe–Mn nodules full separation of the samples' iron from the matrix and especially from copper was only achieved after a further Fe precipitation (see Section 2.3.2). In these cases an exact agreement results from measurements with both methods (Table 6). In fact, experiments on Fe–Mn nodules 1 and 2 (Table 6) revealed that for such samples the SSB is superior to the Cu-doping method in view of accuracy of the data. We emphasise that regardless of the technique used to account for the instrumental mass bias, a high sample purity and absence of any matrix is an unavoidable condition for accurate Fe isotope ratio determinations of natural samples.

3.2.3. Ni-doping

A Ni-doped bracketing technique for instrumental mass bias correction using the ^{61}Ni/^{60}Ni ratio and the Faraday cup setting dubbed "Ni-doping 1" in Table 1 was also tested. With Ni-doping accurate δ^{58}Fe values cannot be obtained due to the large ^{58}Ni interference on ^{58}Fe. However, the determination of ^{58}Fe has no apparent bio- or geochemical application; its significance is probably solely restricted to the determination of mass-independent ^{58}Fe anomalies in some meteorite inclusions [34]. Since the tested Ni-doping method did not require peak jumping the analysis time was equal to that of the SSB method. However, the reproducibility of δ^{56}Fe values of JM Fe with this technique was about twice as large as that for SSB and Cu-doping. This is most likely because measuring uncertainties of the ^{61}Ni/^{60}Ni ratio and thus on the exponential mass bias factor (expressed as factor per atomic mass unit) are propagated into the reproducibility of the corrected ^{56}Fe/^{54}Fe and thus the δ^{56}Fe values by a factor of 2. Another disadvantage of the Ni-doping method is the unfavourable ^{61}Ni/^{60}Ni ratio of only 0.043478. In contrast, the ^{62}Ni/^{60}Ni ratio with a value of 0.128146 and a mass difference of 2 would be more favourable for precise determinations of δ^{56}Fe values of natural samples. However, a dynamic mode with peak jumping would have to be employed using ^{62}Ni/^{60}Ni for instrumental mass bias correction (Table 1) and thus there would be no real advantage over the Cu-doping method.

4. Discussion and conclusions

Our detailed analysis of the methodological pitfalls suggests that avoiding matrix effects, introduced by extraneous metals, organic substances, inaccurate acid concentrations, changing Fe speciation in solution or widely varying Fe concentrations, presents the most formidable challenge in Fe isotope analysis. Such matrix effects can shift the instrumental mass discrimination in a cryptic manner, and might easily be misinterpreted as samples' real isotope fractionation [14]. Mass spectrometric duplicates would not necessarily identify these artefacts, given that they are likely to reproduce. The essential prerequisite for any Fe isotope ratio analysis is that the sample has the highest possible purity, and that it is in a chemical form that matches exactly that of the standard used for instrumental mass bias acquisition.

If these conditions are met, then Fe isotope results from standard-sample bracketing (SSB) are identical to those that were corrected with Cu-doping. This demonstrates that highest achievements can be met with or without doping (B. Icyclette and S. Printer, pers. comm., summer 2004). We did not observe the inferior reproducibility for δ^{56}Fe values of natural samples when using SSB compared to Cu-doping that was reported by Arnold et al. [25]. However, it is agreed that with the Cu-doping technique some cryptic matrix effects might in some cases be detected that would go unnoticed with SSB. One advantage of Cu-doping is that it enables accurate results during unstable mass spectrometric conditions (e.g. during the warm-up phase) whereas SBB requires fully stable instrumental conditions. On the other hand, the mass bias between Cu and that of Fe is not constant, which requires standard bracketing even with Cu-doping. A clear disadvantage of Cu-doping is therefore the increased analytical time required, which is double that of the pure SSB method.

Double spiking is a third technique that would potentially correct for instrumental mass discrimination. The advantage is that incomplete recovery during chemical processing likely to produce an isotope fractionation is also taken into account. For Fe analysis, however, chemical processing is usually straightforward; a combination of anion exchange and hydroxide precipitation ensures complete recovery and highest sample purity. Therefore, double spiking appears unnecessary for Fe isotope analysis. A clear disadvantage of the double-spike method for Fe isotope determinations is that inaccuracies in the correction of isobaric interferences cannot be identified in δ^{56}Fe versus δ^{57}Fe diagrams.

In hundreds of Cu-free SSB analyses, an external 95% confidence level for natural samples has been achieved of 0.049, 0.071 and 0.28‰, for the δ^{56}Fe, δ^{57}Fe and δ^{58}Fe values, respectively. This external reproducibility of natural samples is identical to the pure mass spectrometric reproducibility of the synthetic JM Fe standard of 0.046, 0.073 and 0.41‰ for the δ^{56}Fe, δ^{57}Fe and δ^{58}Fe values, respectively. Therefore, Cu-free standard-sample bracketing SSB is our preferred method of choice (see [35]).

4.1.1. Data acceptance criteria

A routine analytical protocol summarised below was employed to identify and avoid analytical pitfalls and to introduce an essential level of quality control. While the development of this protocol is based on the results discussed in this work, some of our limits for data rejection may be more stringent than required by our experiments.

(1) To ensure complete recovery of Fe during chemical purification by anion exchange chromatography, the total amount of loaded Fe must not exceed a small fraction of the resin's capacity.
(2) Uncommon sample matrix types are tested by repeated chemical processing of the same sample aliquot and by replicate measurements of chemical aliquots. Replicates should agree within the general reproducibility limits. Furthermore, the matrix test with synthetic Fe-doping lined out in this study is performed for such novel sample types. Synthetic Fe results of such matrix tests need to be within the uncertainty limits determined on the unprocessed synthetic Fe solutions.
(3) Concentrations of Fe analytes of natural samples must be matched to that of the bracketing Fe standard. The concentrations should lie within the limits determined not to affect the instrumental mass bias or cancelling out of residual interferences (see Fig. 4). To safely avoid any artefacts, we set the signal limits of samples to within ±10% of their bracketing IRMM-014 Fe standards.
(4) We check the separated Fe of all samples for purity by optical ICP measurement prior to isotope analysis. Should impurities still exist after one anion exchange pass, samples are subjected to further chemical purification by either a second anion exchange pass or hydroxide precipitation.
(5) Fe data of natural samples that encounter ^{54}Cr/^{54}Fe ratios exceeding 0.1‰ are rejected. If a sample ^{58}Ni/^{58}Fe ratio exceeds 1%, the reliability of the δ^{58}Fe value for the sample is regarded questionable.
(6) Fe isotope data of samples is accepted only if the Fe isotope composition of a known Fe standard measured repeatedly in the same analysis session is within the uncertainty limits given in Table 2.
(7) Fe isotope data of natural samples that do not overlap the mass-dependent fractionation line in δ^{57}Fe versus δ^{56}Fe space within their 95% confidence error ellipses are rejected as analytical outliers.
(8) A sample for which the two directly bracketing standard measurements exceed an instrumental mass bias drift of 200 ppm on the ^{56}Fe/^{54}Fe ratio is rejected.

Acknowledgements

We are greatly indebted to Ken Ludwig for helpful information about calculating error ellipses and overall statistical treatment of our data. We thank Marc Mamberti and Ingo Horn for laboratory assistance. Thomas Walczyk, Carol Frost, and two anonymous referees are thanked for comments that helped to improve the manuscript. This work was supported by DFG grant BL 561-1.

Appendix A. Supplementary data

Supplementary data associated with this article can be found, in the online version, at doi:10.1016/j.ijms.2004.11.025.

References

[1] E.A. Schauble, G.R. Rossmann, H.P. Taylor, Geochim. Cosmochim. Acta 65 (2001) 2487.
[2] V.B. Polyakov, Geochim. Cosmochim. Acta 61 (1997) 4213.
[3] V.B. Polyakov, S.D. Mineev, Geochim. Cosmochim. Acta 64 (2000) 849.
[4] A.D. Anbar, Trans. Am. Geophys. Union 82 (2001) 173.
[5] B.L. Beard, C.J. Johnson, K.L. Von Damm, R.L. Poulson, Geology 31 (2003) 629.
[6] T.D. Bullen, A.F. White, C.W. Childs, D.V. Vivit, M.S. Schulz, Geology 29 (2001) 699.
[7] T. Walczyk, F. von Blanckenburg, Science 295 (2002) 2066.
[8] X.K. Zhu, R.K. O'Nions, Y. Guo, B. Reynolds, Science 287 (2000) 2001.
[9] C.M. Johnson, J.L. Skulan, B.L. Beard, H. Sun, K.H. Nealson, P.S. Braterman, Earth Planetary Sci. Lett. 195 (2002) 141.
[10] J. Völkening, D.A. Papanastassiou, Astrophys. J. 347 (1989) 43.
[11] P.R. Dixon, R.E. Perrin, D.J. Rokop, R. Maeck, D.R. Janecky, J.P. Banar, Anal. Chem. 65 (15) (1993) 2125.
[12] T. Walczyk, Int. J. Mass Spectrom. 161 (1997) 217.
[13] C.M. Johnson, B.L. Beard, Int. J. Mass Spectrom. 193 (1999) 87.
[14] B.L. Beard, C.M. Johnson, J.L. Skulan, K.H. Nealson, L. Cox, H. Sun, Chem. Geol. 195 (2003) 87.
[15] N.S. Belshaw, X.K. Zhu, Y. Guo, R.K. O'Nions, Int. J. Mass Spectrom. 197 (2000) 191.
[16] C.N. Maréchal, P. Télouk, F. Albarède, Chem. Geol. 156 (1999) 251.
[17] A. Galy, N.S. Belshaw, L. Halicz, R.K. O'Nions, Int. J. Mass Spectrom. 208 (2001) 89.
[18] C. Siebert, T.F. Nägler, J.D. Kramers, Determination of molybdenum isotope fractionation by double spike multicollector inductively coupled plasma mass spectrometry, geochemistry, geophysics, Geosystems 2, 2000GC000124, 2001.
[19] A.D. Anbar, J.E. Roe, J. Barling, K.H. Nealson, Science 288 (2000) 126.

[20] K. Kehm, E.H. Hauri, C.M.O. Alexander, R.W. Carlson, Geochim. Cosmochim. Acta 67 (2003) 2879.
[21] S. Weyer, J. Schwieters, Int. J. Mass Spectrom. 226 (2003) 355.
[22] A. Stenberg, D. Malinovsky, I. Rodushkin, H. Andrén, C. Pontér, B. Öhlander, D.C. Baxter, J. Anal. Atom. Spectrom. 18 (2003) 23.
[23] D. Malinovsky, A. Stenberg, I. Rodushkin, H. Andrén, J. Ingri, B. Öhöander, D.C. Baxter, J. Anal. Atom. Spectrom. 18 (2003) 687.
[24] A.N. Halliday, P.A. Freedman, F. Oberli, H. Baur, S. Hollins, S. Levasseur, I. Leya, F. Poitrasson, G. Quitte, N. Teutsch, U. Wiechert, H. Williams, J. Williams, Geochim. Cosmochim. Acta 66 (15A) (2002) A303.
[25] G.L. Arnold, S. Weyer, A.D. Anbar, Anal. Chem. 76 (2) (2004) 322.
[26] P.D.P. Taylor, R. Maeck, P. DeBievre, Int. J. Mass Spectrom. Ion Proc. 121 (1992) 111.
[27] P.D.P. Taylor, R. Maeck, F. Hendrickx, P. Debievre, Int. J. Mass Spectrom. Ion Process. 128 (1–2) (1993) 91.
[28] W.M. White, F. Albarede, P. Telouk, Chem. Geol. 167 (3–4) (2000) 257.
[29] J.B. Schwieters, M. Hamester, G. Jung, R. Pesch, L. Rottman, S. Weyer, in: EUG 590, 2000.
[30] K.R. Ludwig, D.M. Titterington, Geochim. Cosmochim. Acta 58 (22) (1994) 5031.
[31] K.R. Ludwig, in: B. Bourdon, G.M. Henderson, C.C. Lundstrom, S.P. Turner (Eds.), Uranium-Series Geochemistry, Reviews in Mineralogy and Geochemistry, vol. 52, 2003, pp. 631–656.
[32] W.H. Press, S.A. Teukolsky, W.T. Vetterling, B.P. Flannery, Numerical Recipes in Fortran, Cambridge University Press, Cambridge, 1992.
[33] F. Albarède, B.L. Beard, in: C.M. Johnson, B.L. Beard, F. Albarède (Eds.), Geochemistry of Non-Traditional Stable Isotopes, Reviews in Mineralogy and Geochemistry, vol. 55, Mineralogical Society of America, Blacksburg, 2004, pp. 113–152.
[34] J. Volkening, D.A. Papanastassiou, Astrophys. J. 347 (1) (1989) 43.
[35] T. Walczyk, F. von Blanckenburg, Deciphering the iron isotope message of the human body, Int. J. Mass Spectrom., 242 (2005) 117.